Non-dipolar magnetospheric accretion & redshifted absorption in HeI 10830 Å

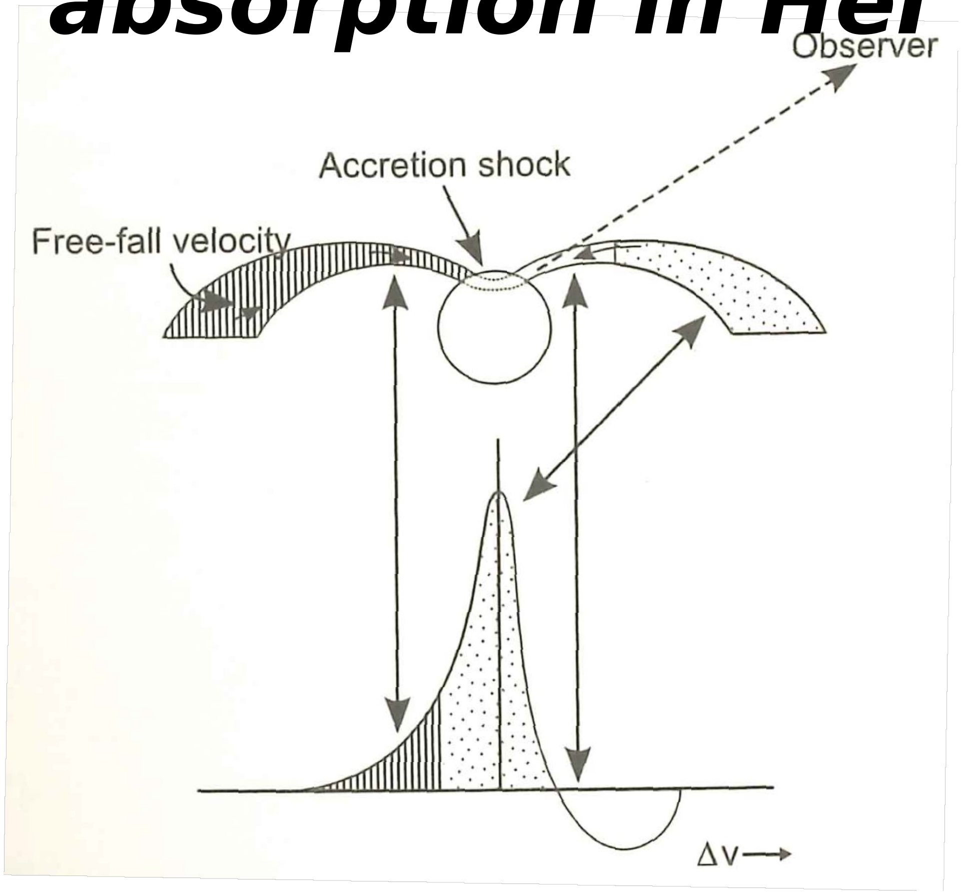

Accretion-related emission line profile
Calvet & D'Alessio 2011

Scott G. Gregory

University of St Andrews | FOUNDED 1413

HeI 10830Å as an accretion diagnostic

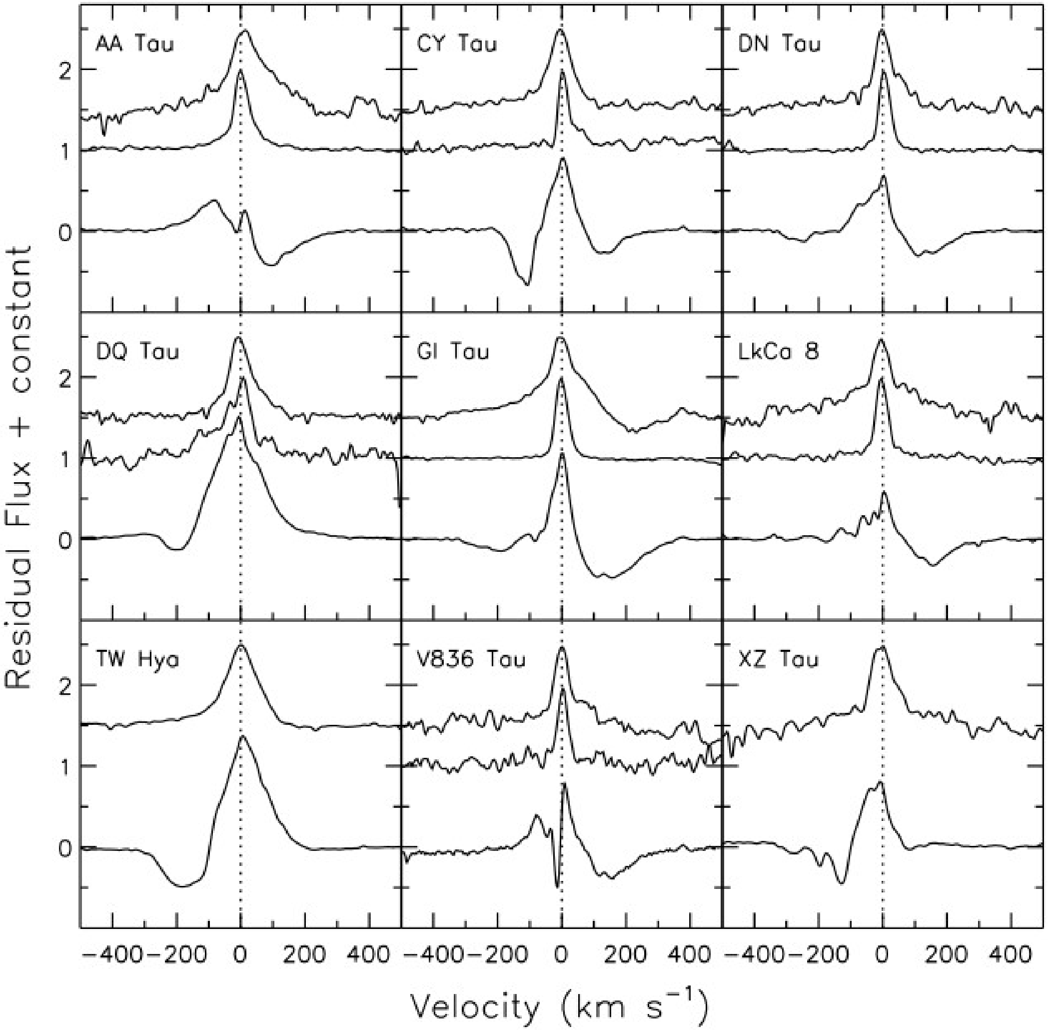

(Edwards et al 2006)

- (*top to bottom*) Pγ, HeI 5876Å (when available), HeI 10830Å.
- 10830Å is a more sensitive probe of accretion; subcontinuum redshifted absorption is more common.

Models of redshifted absorption in HeI 10830Å with dipole magnetospheres – Fischer et al 2008

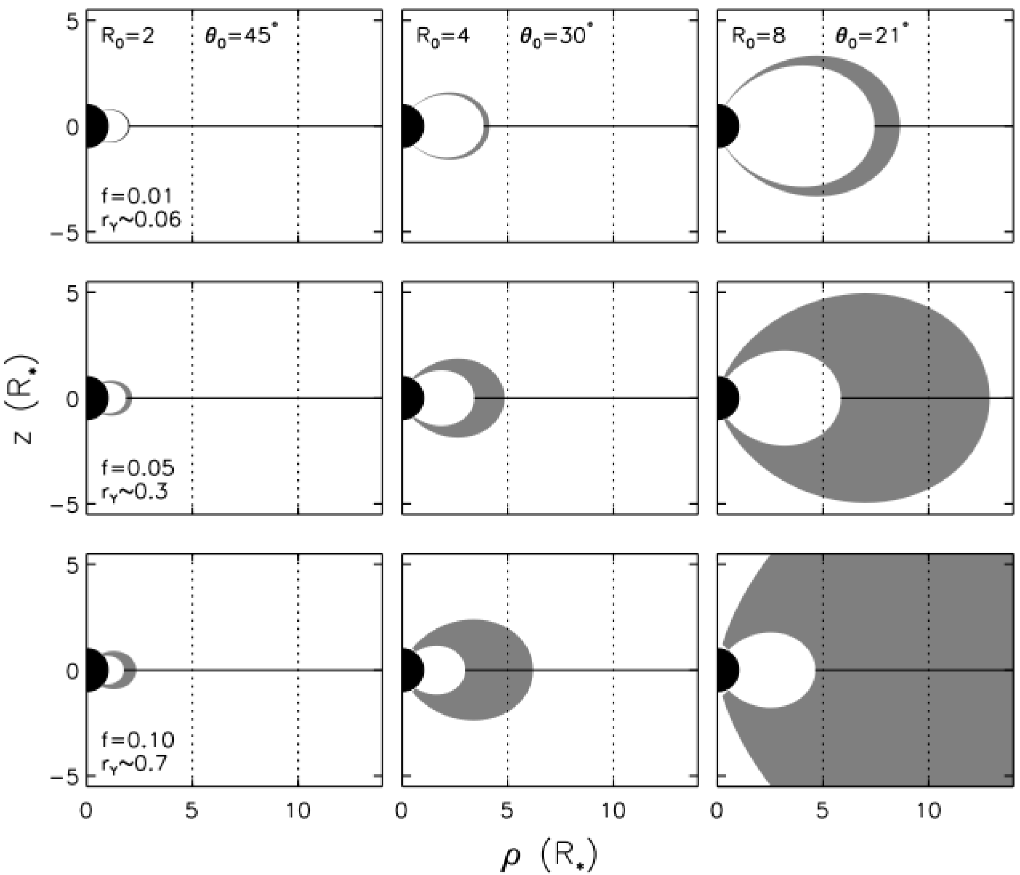

- To explain the breadth of the red absorption, wide accretion columns often required – resulting in large hotspots & too much veiling.

- Introduced the idea of “accretion streamlets” – dilute columns of accretion

The stellar internal structure evolves as stars follow their mass tracks …ards the main seque…

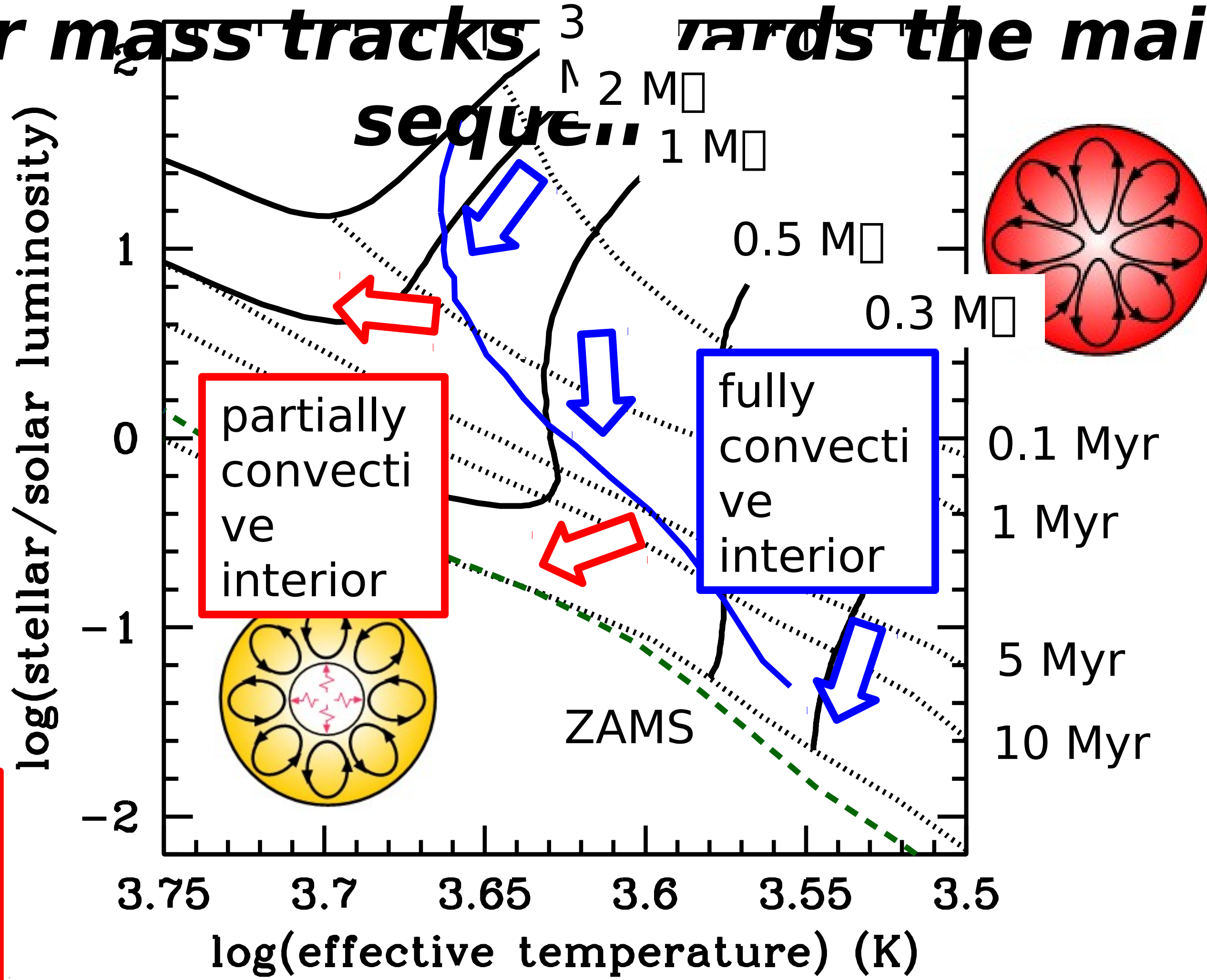

radiative core, convective outer envelope

(Gregory et al 2012, 2014 – magnetic Hertzsprung-Russell diagram)

Are Sun-like stars born with simple B-fields that become more complex as they contract und

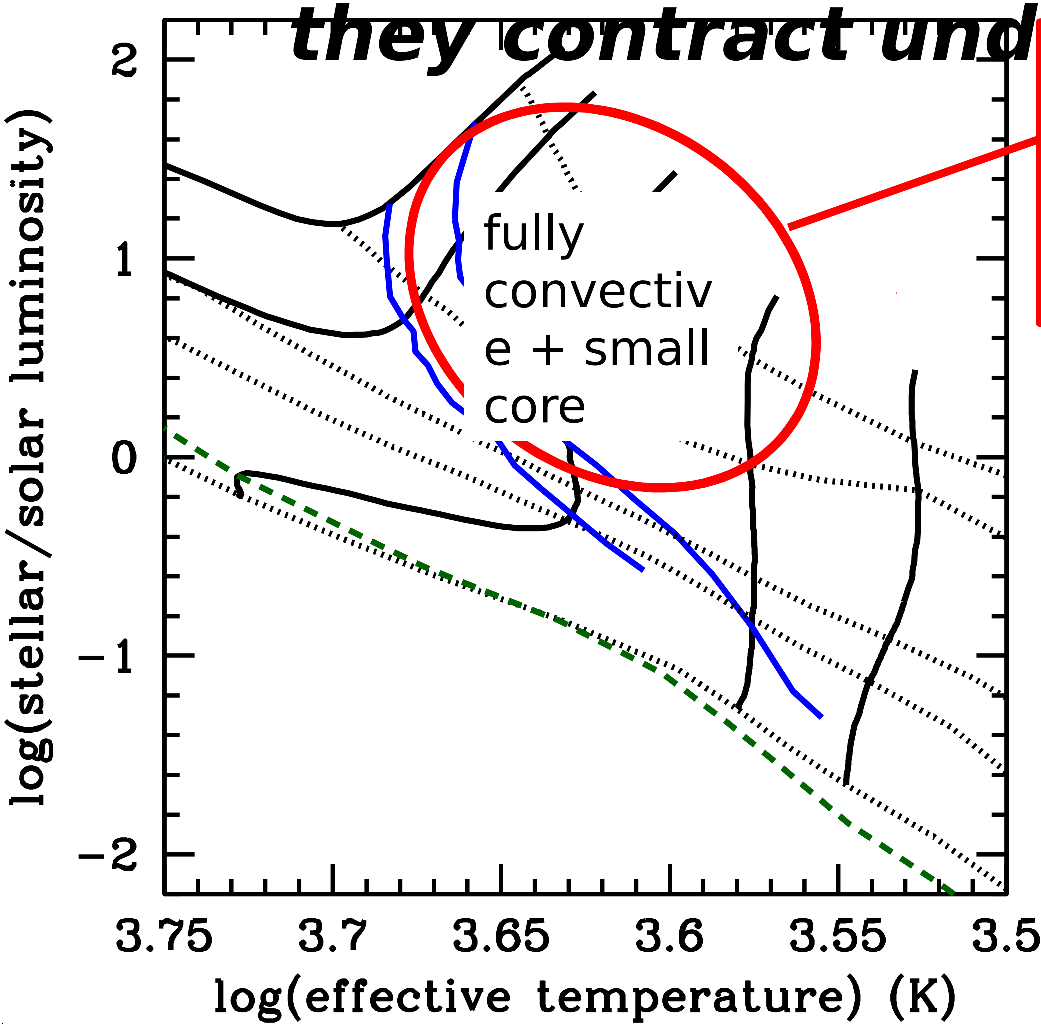

Gregory et al 2012, 2014 –
magnetic Hertzsprung-Russell diagram

simple axisymmetric large-scale magnetic fields (dipole or octupole modes dominate)

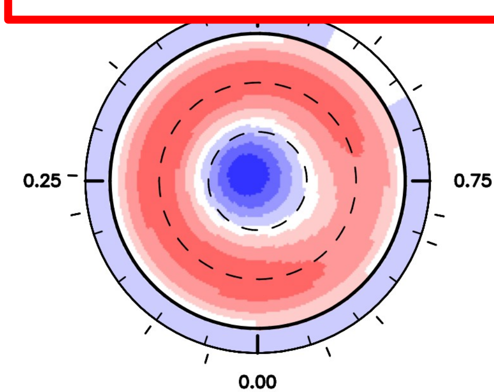

(Donati et al 2010a, 2011a)

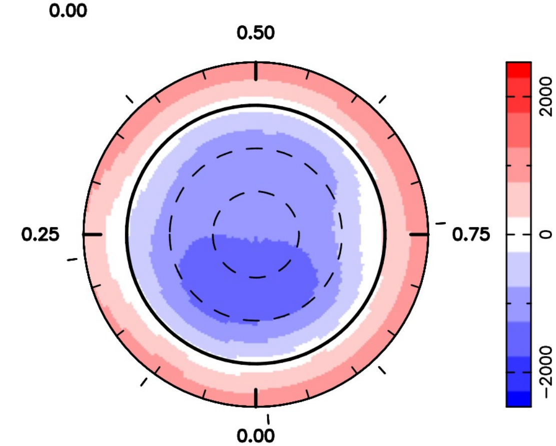

Are Sun-like stars born with simple B-fields that become more complex as they contract und

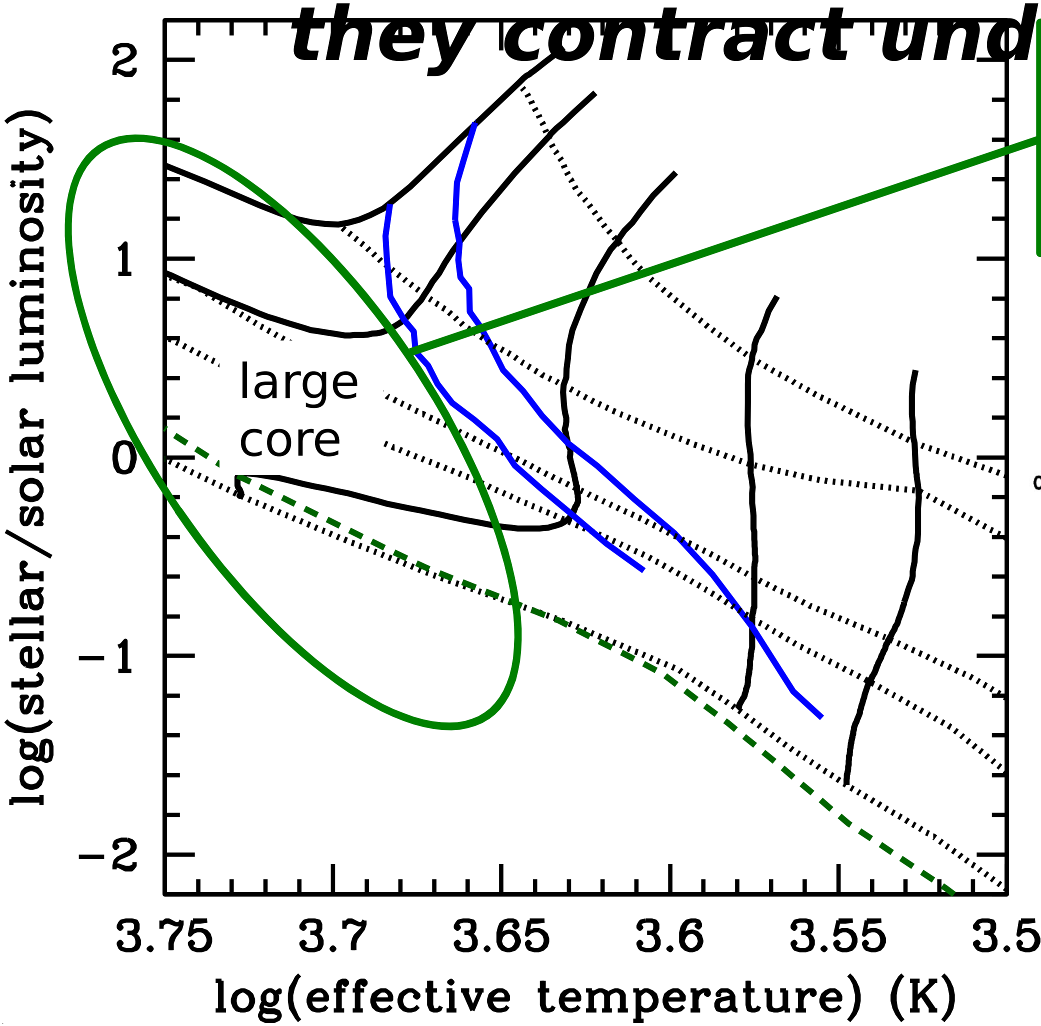

Gregory et al 2012 –
magnetic Hertzsprung-Russell diagram

complex, messy, non-axisymmetric large-scale magnetic fields

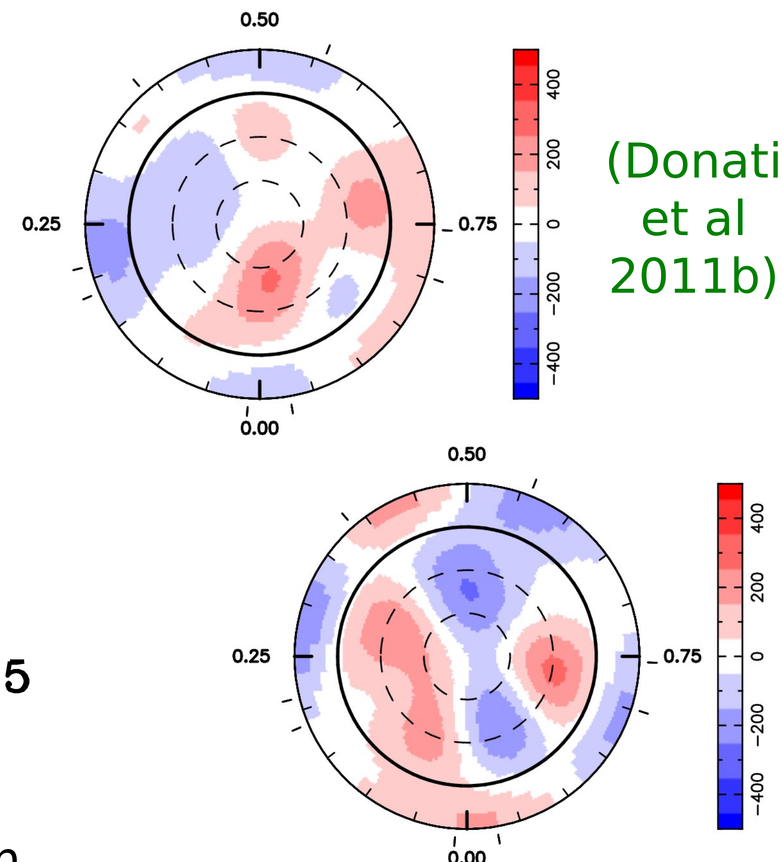

(Donati et al 2011b)

Large-scale magnetic fields of accreting PMS stars become more dominantly octupolar with age

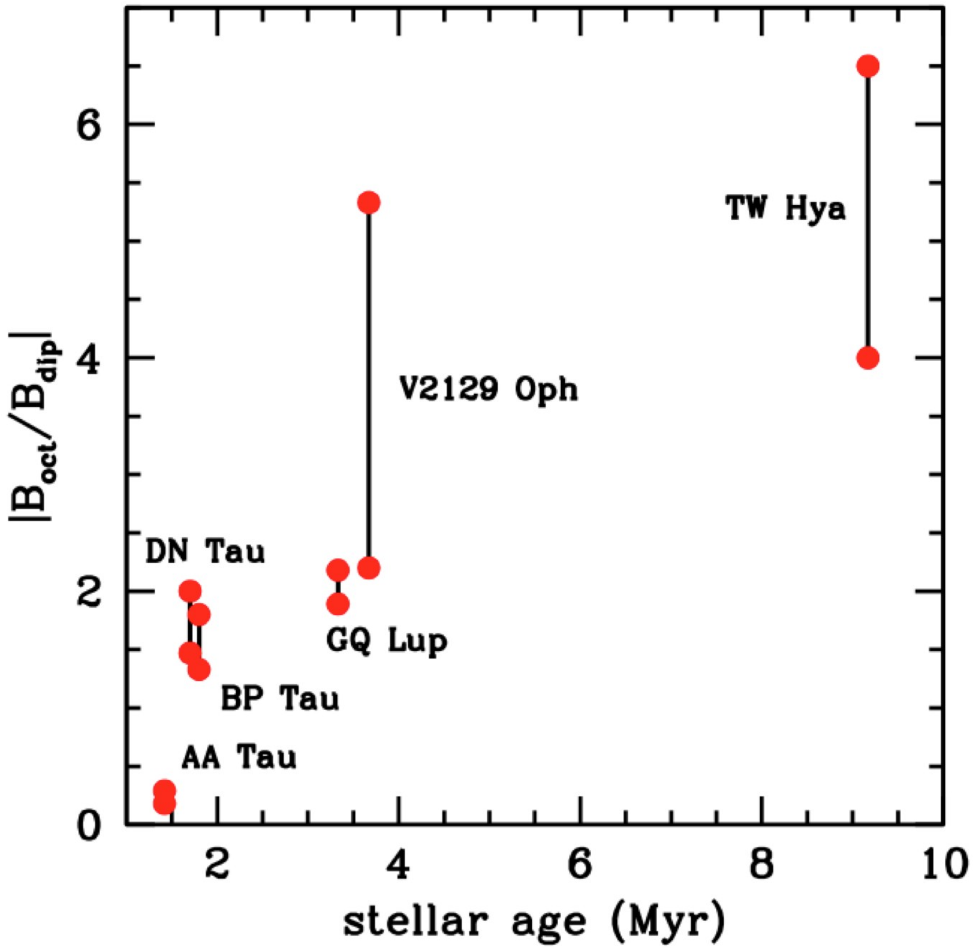

(Gregory et al 2014; Donati et al 2007,08,10,11a,b,12,13)

- Dipole and octupole (plus other) moments vary in strength, tilt, and phase of tilt, year-to-year.

Accreting PMS stars with ~dipole + octupole magnetic fields

Star	Date	Bdip (kG)	Dipole tilt	Phase dip tilt	Boct (kG)	Octupole tilt	Phase oct tilt	Boct/Bdip
AA Tau	Jan09	1.7	**170o**	0.65	0.5	**10o**	0.5	0.3
BP Tau	Feb06	1.2	**20o**	0.65	1.6	**10o**	0.15	1.3
GQ Lup	Jun11	0.9	**30o**	0.05	1.6	**0o**	-	1.8
DN Tau	Dec12	0.3	**25o**	0.9	0.6	**0o**	-	2.0
V2129 Oph	Jul09	1.0	**15o**	0.4	2.2	**20o**	0.5	2.2
TW Hya	Mar10	0.7	**5o**	0.25	2.8	**>175o**	0.85	4.0

- Tilt is the location of the main positive pole relative to the visible stellar rotation pole (updated from Gregory & Donati 2011).

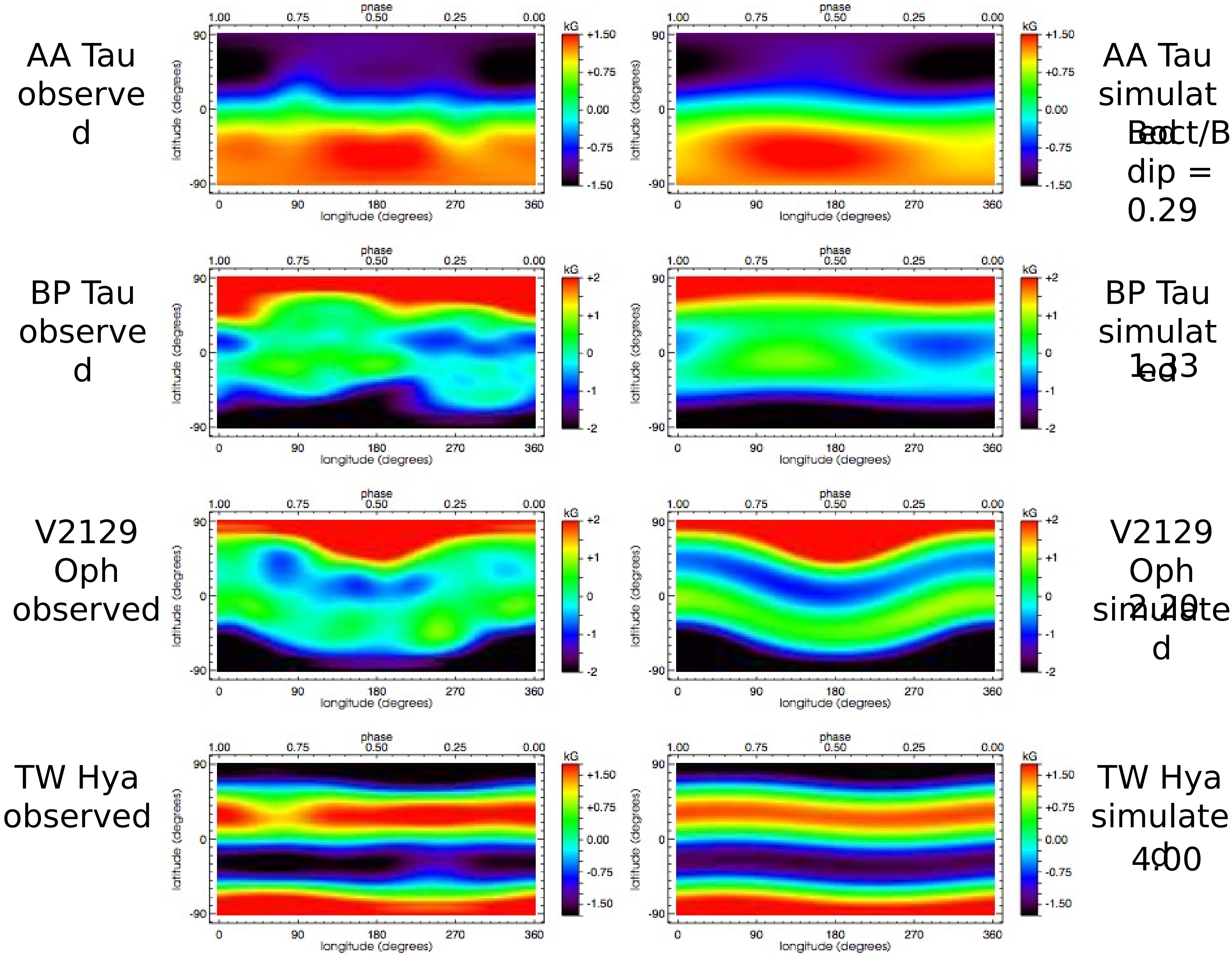
AA Tau observed
AA Tau simulated
Boct/B dip = 0.29
BP Tau observed
BP Tau simulated
1.33
V2129 Oph observed
V2129 Oph simulated
2.20
TW Hya observed
TW Hya simulated
4.00
phase
longitude (degrees)
latitude (degrees)
kG

Axisymmetric dipole & octupole magnetic fields

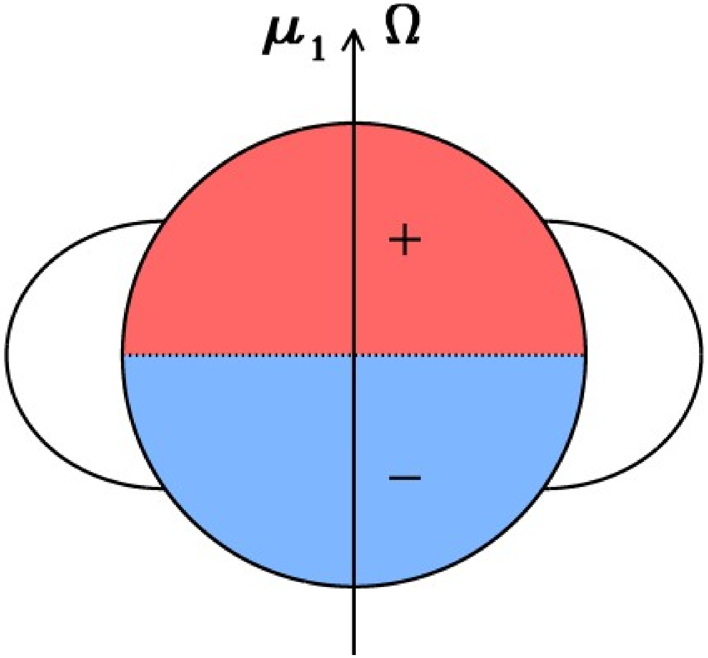

l = 1, m = 0

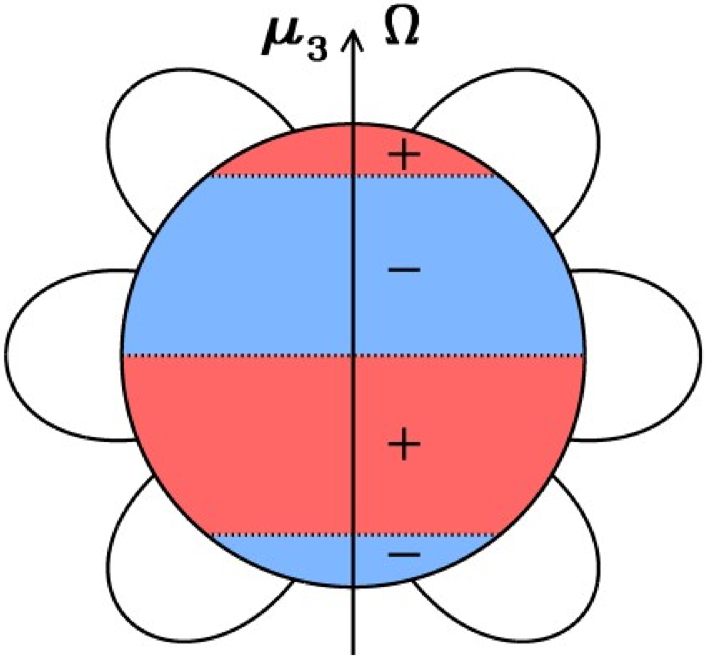

l = 3, m = 0

Parallel dipole & octupole moments

Axisymmetric dipole & octupole magnetic fields

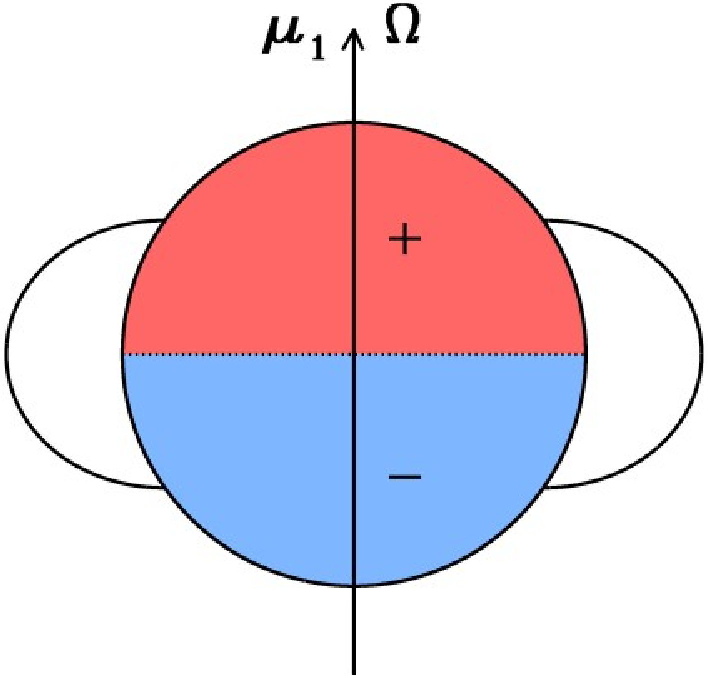

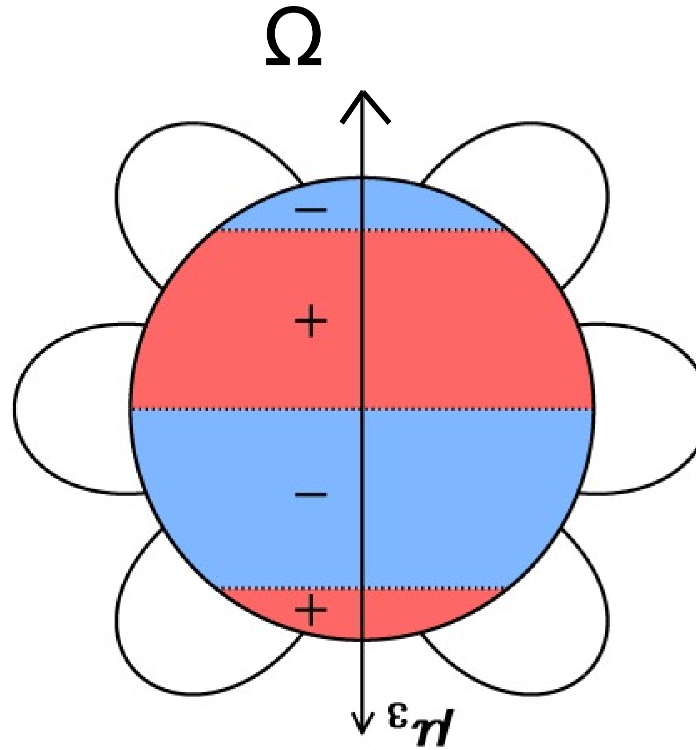

l = 1, m = 0

l = , m = 0

Anti-parallel dipole & octupole moments

Axisymmetric dipole + octupole magnetic fields

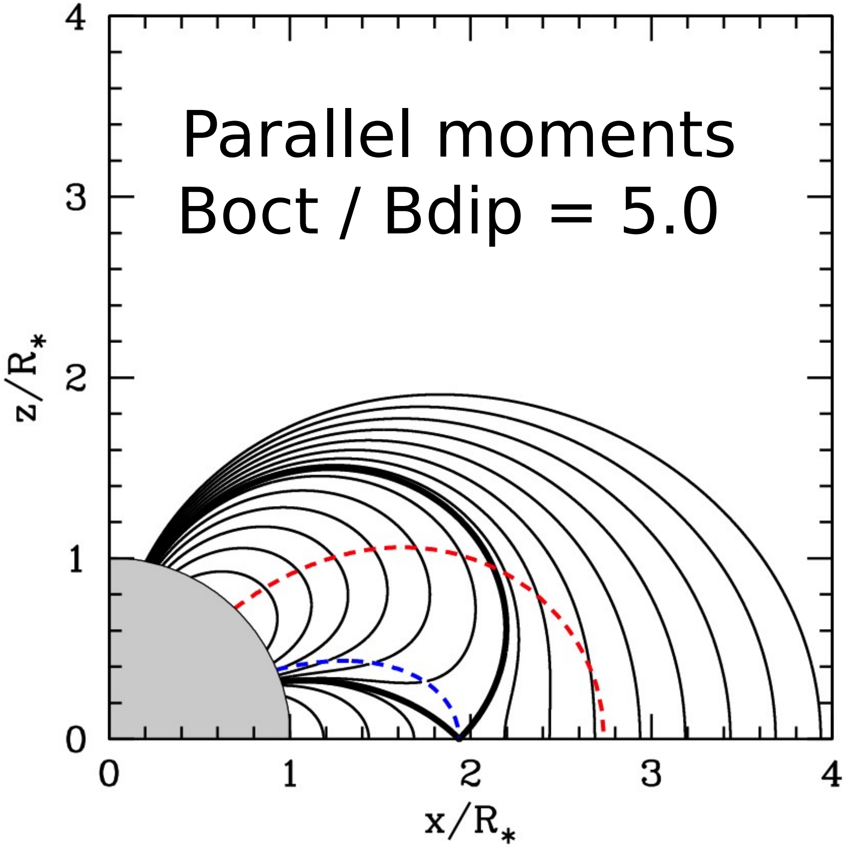

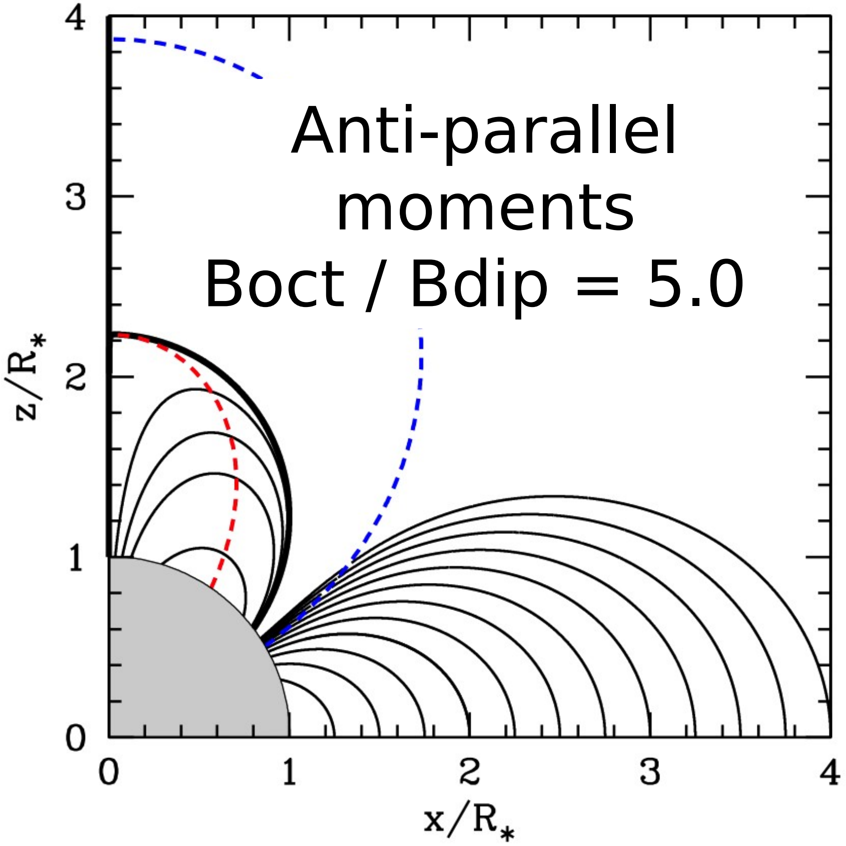

(Gregory, Fischer & Hillenbrand, in prep.)

Dipole + octupole magnetic null point

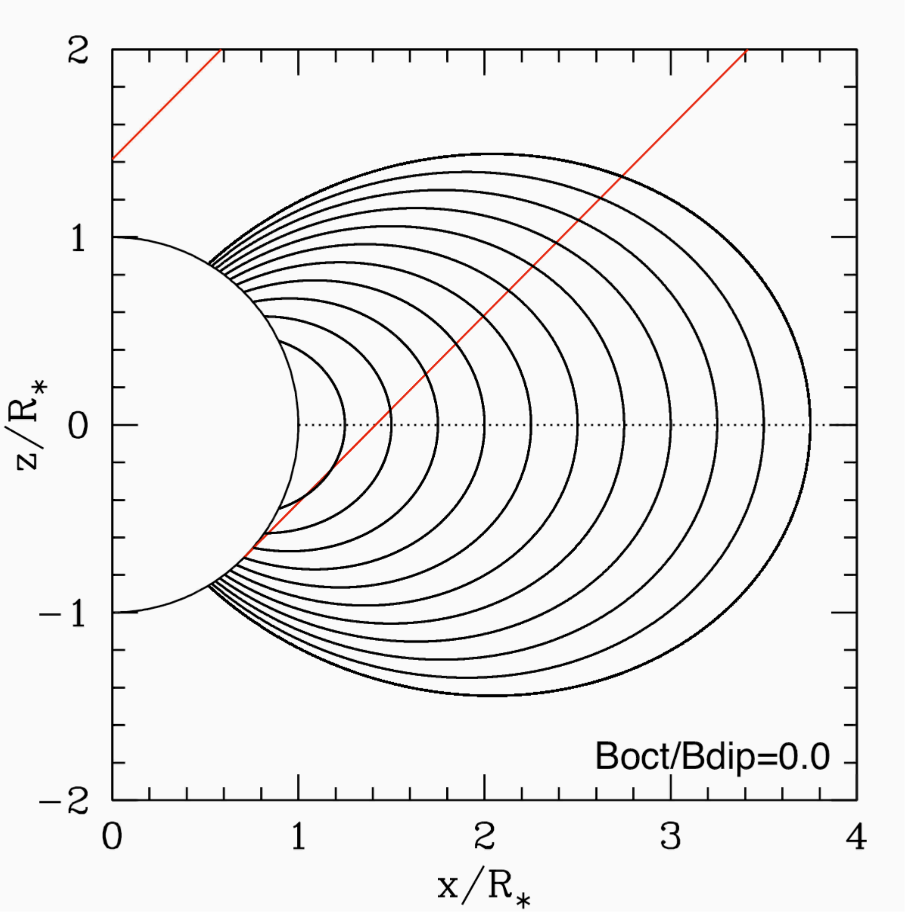

- The magnetic topology depends on the ratio of the polar field strengths Boct/Bdip.
- Magnetic null point:

$$r_{null} = \left(\frac{3}{4} \frac{B_{oct}}{B_{dip}} \right)^{1/2} R_*$$

- Equatorial shell of closed field only exists when Boct/Bdip > 4/3.

Disk truncation with dipole + octupole fields

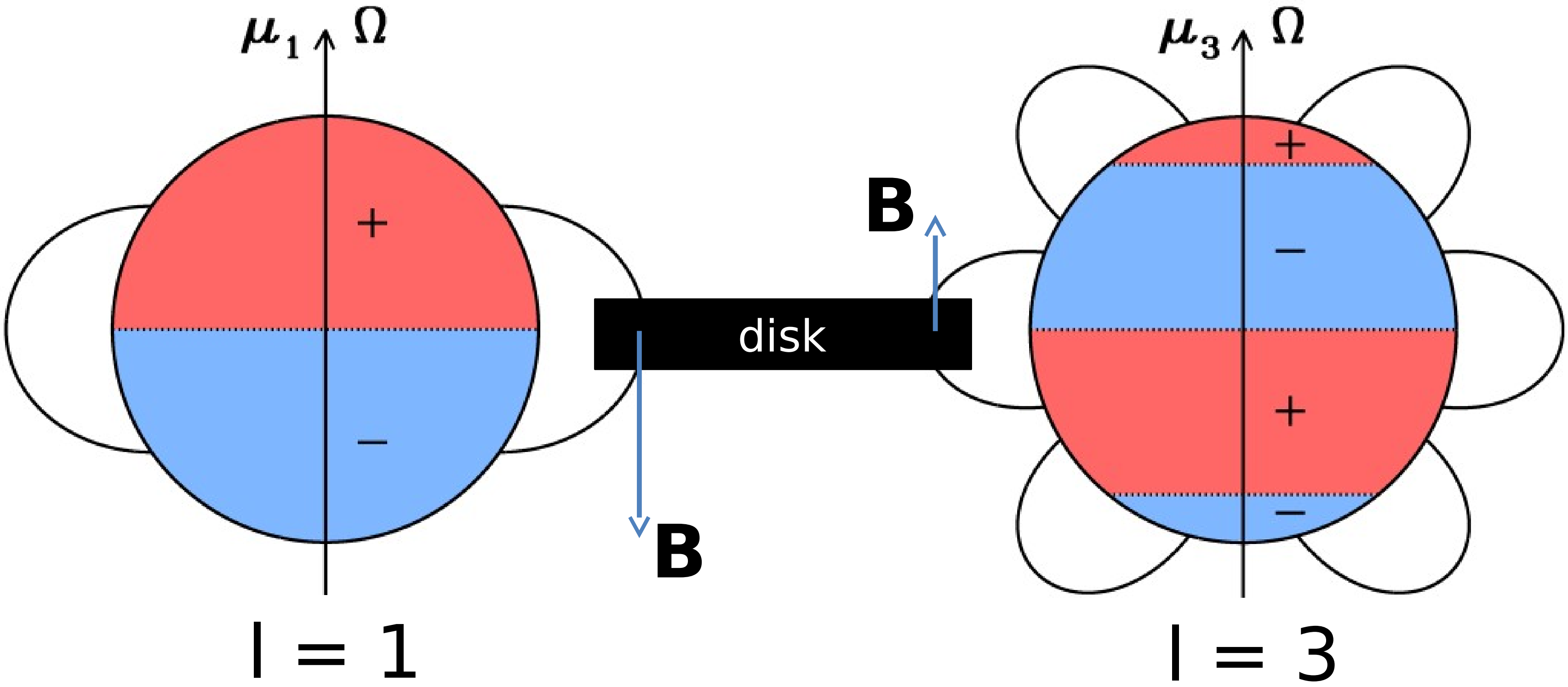

- Parallel (anti-parallel) moments, Bz at inner disk smaller (larger) than the dipole case: disk truncated closer (farther) from the star.

Disk truncation with dipole + octupole fields

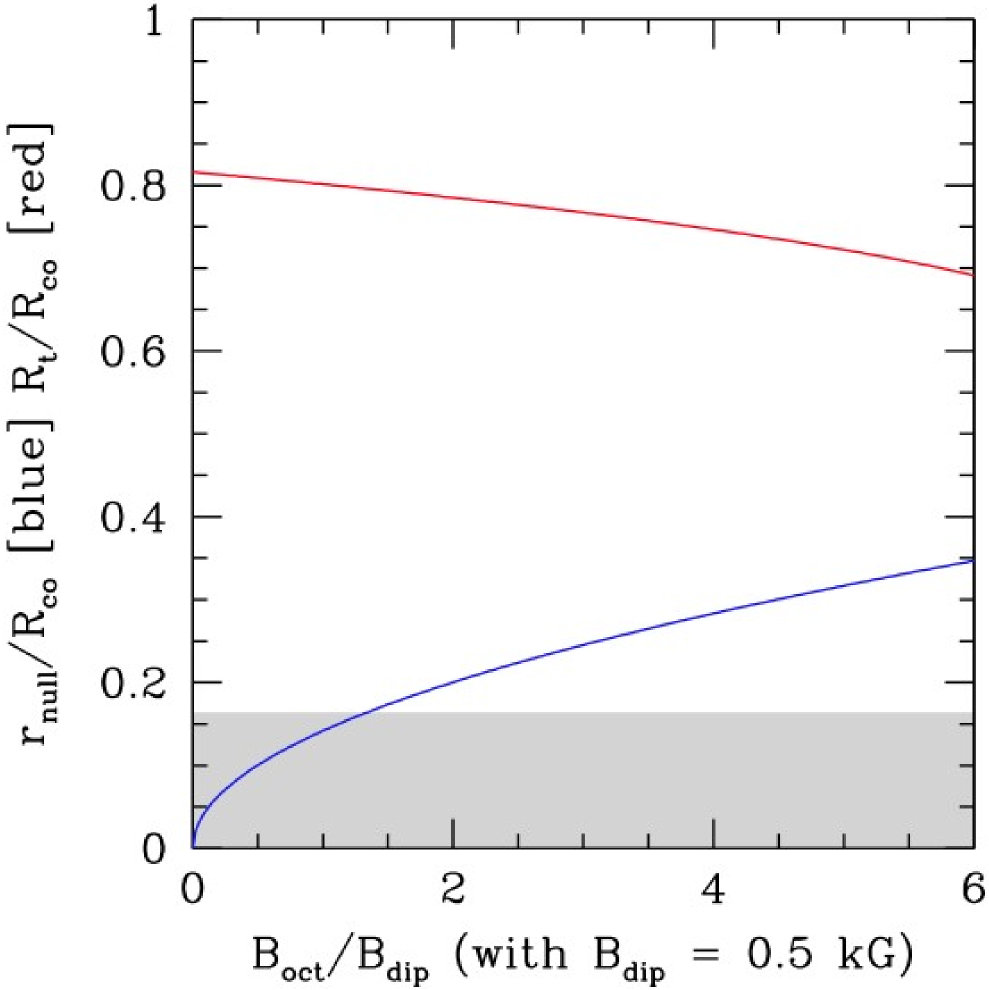

(see also Adams & Gregory 2012; Johnston et al 2014)

- The stronger the octupole relative to the dipole the closer the disk is to the star for ~parallel moments.
- Disk farther from the star if moments ~anti-parallel.
- Truncation dominated by the dipole part of the field.

Accretion flow/spots with dipole + octupole fields

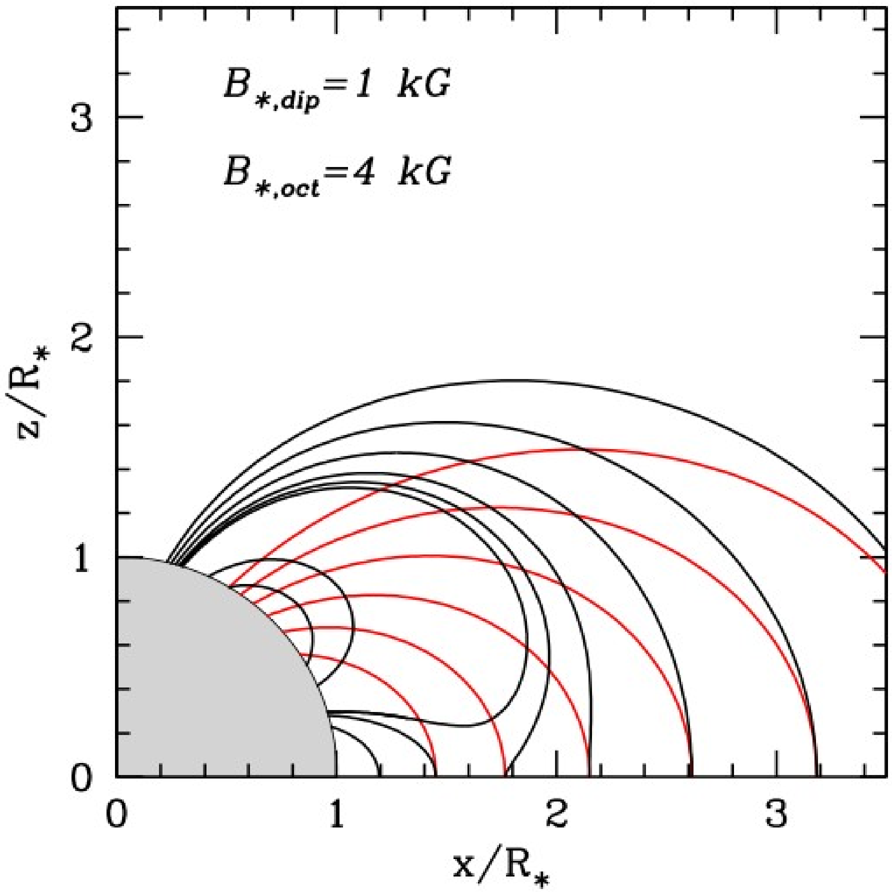

(Gregory, Fischer & Hillenbrand, in prep.)

- Accretion column is "squeezed" by the complex surface field.
- Higher (lower) latitude accretion spots compared to a dipole for parallel (anti-parallel) moments.
- Higher pre-shock densities (e.g. Gregory et al 2007).

Smaller, denser, hotter accretion spot & less veiling with dipole + octupole fields

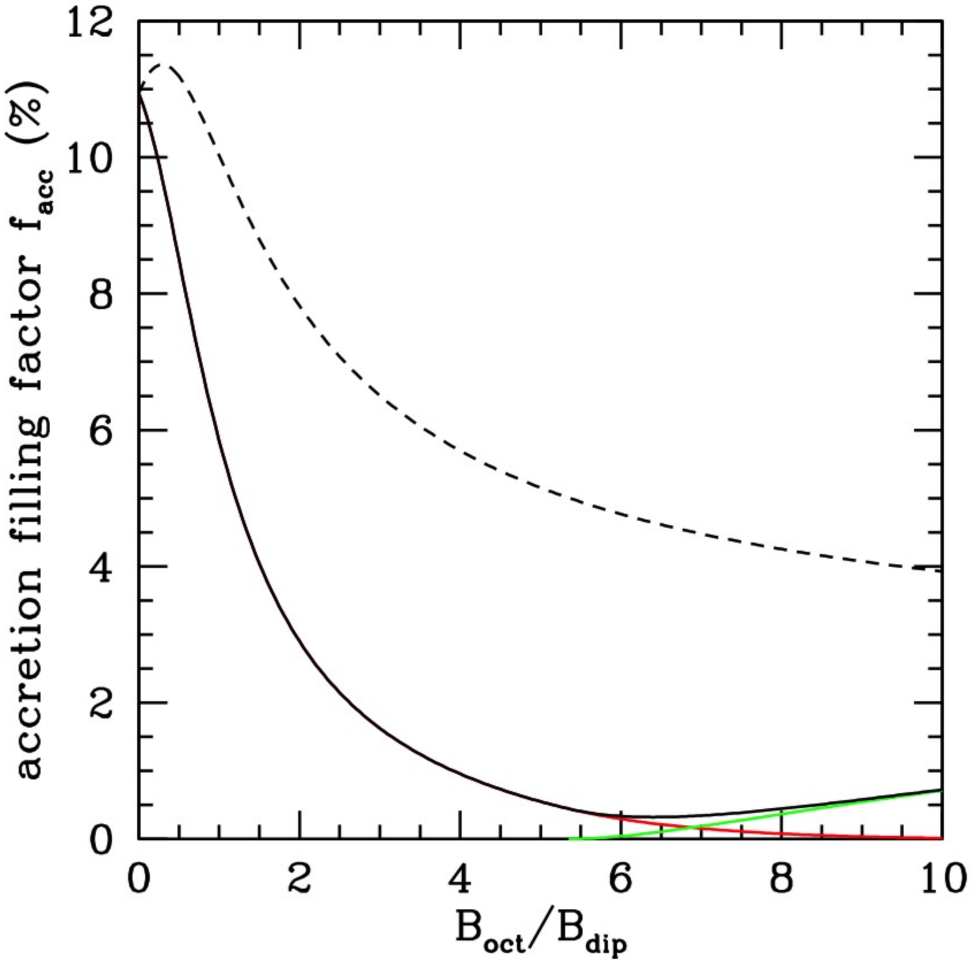

(Gregory, Fischer & Hillenbrand, in prep.)

- Hot spot covering fraction lower for non-dipole fields.
- Surface field squeezes large scale field.
- Veiling is reduced relative to the dipole case; temperature & density are increased.

Smaller, denser, hotter accretion spot & less veiling with dipole + octupole fields

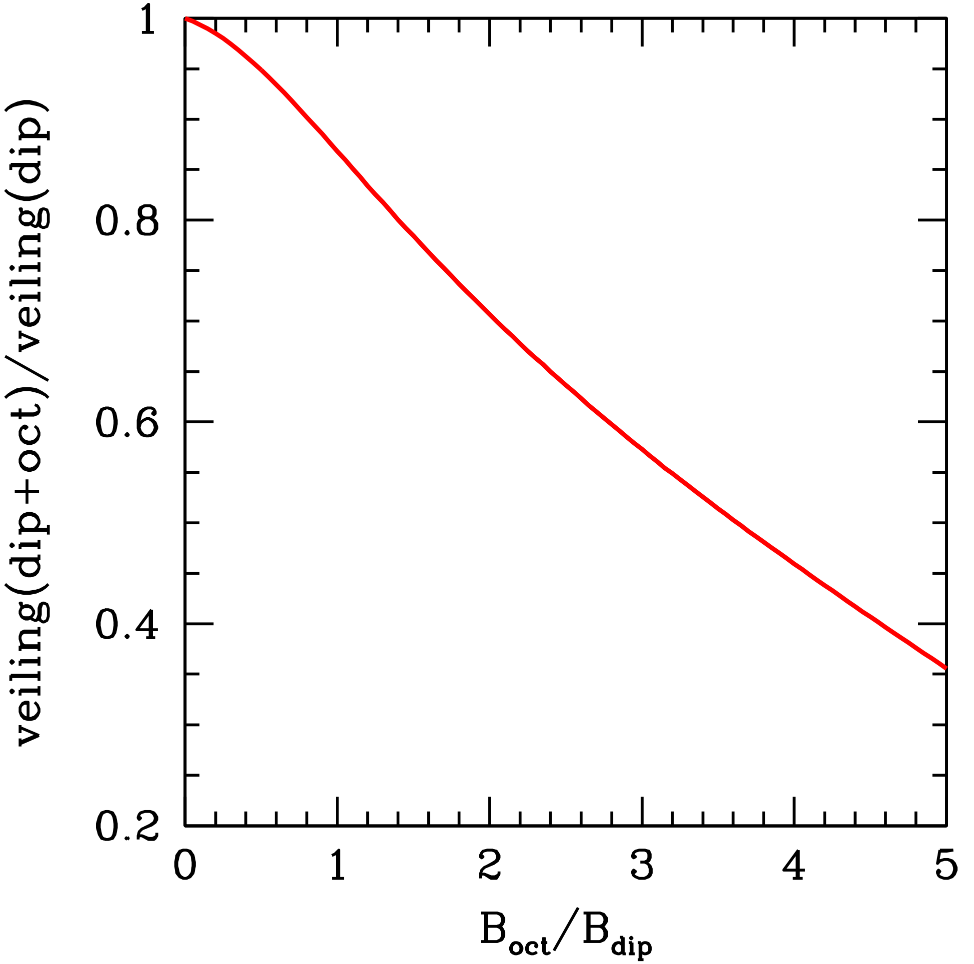

(Gregory, Fischer & Hillenbrand, in prep.)

- Hot spot covering fraction lower for non-dipole fields.
- Surface field squeezes large scale field.
- Veiling is reduced relative to the dipole case; temperature & density are increased.

Smaller, denser, hotter accretion spot & less veiling with dipole + octupole fields

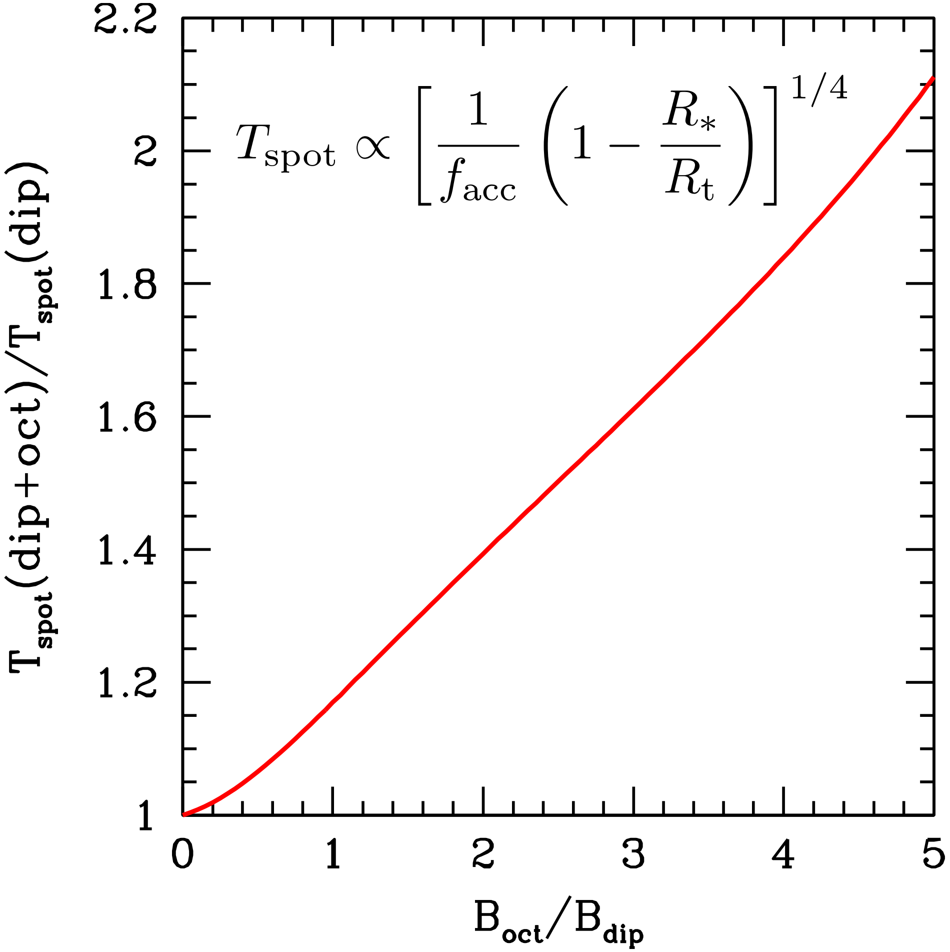

(Gregory, Fischer & Hillenbrand, in prep.)

- Hot spot covering fraction lower for non-dipole fields.
- Surface field squeezes large scale field.
- Veiling is reduced relative to the dipole case; temperature & density are increased.

Subcontinuum absorption at HeI 10830Å

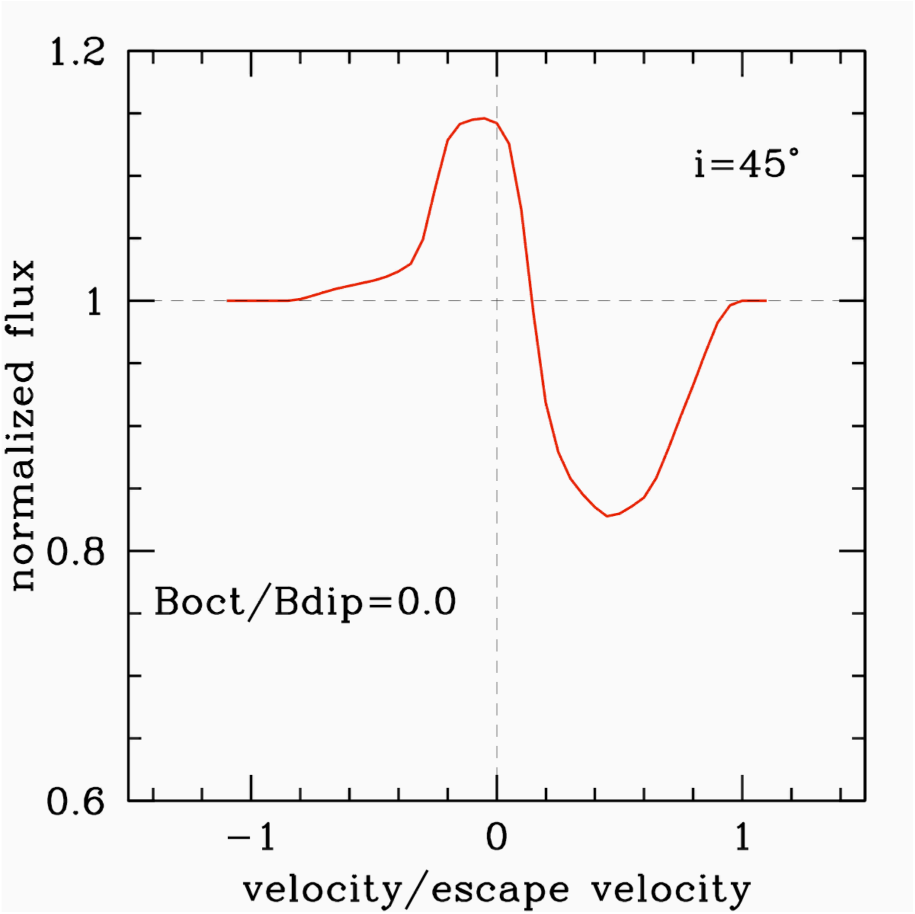

(Gregory, Fischer & Hillenbrand, in prep)

- Red line = dipole; black line = dipole+octupole.
- Updated from Fischer et al (2008)
- Analysis of redshifted absorption components can produce erroneous parameters if the magnetic topology is unknown.

Summary

- ~half of the accreting PMS stars with derived magnetic maps have large-scale magnetospheres that are well described by a tilted dipole plus a titled octupole component.

- Field geometry controls the shape, size, temperature, and density of accretion spots.

- Subcontinuum redshifted absorption influenced by the magnetic topology.

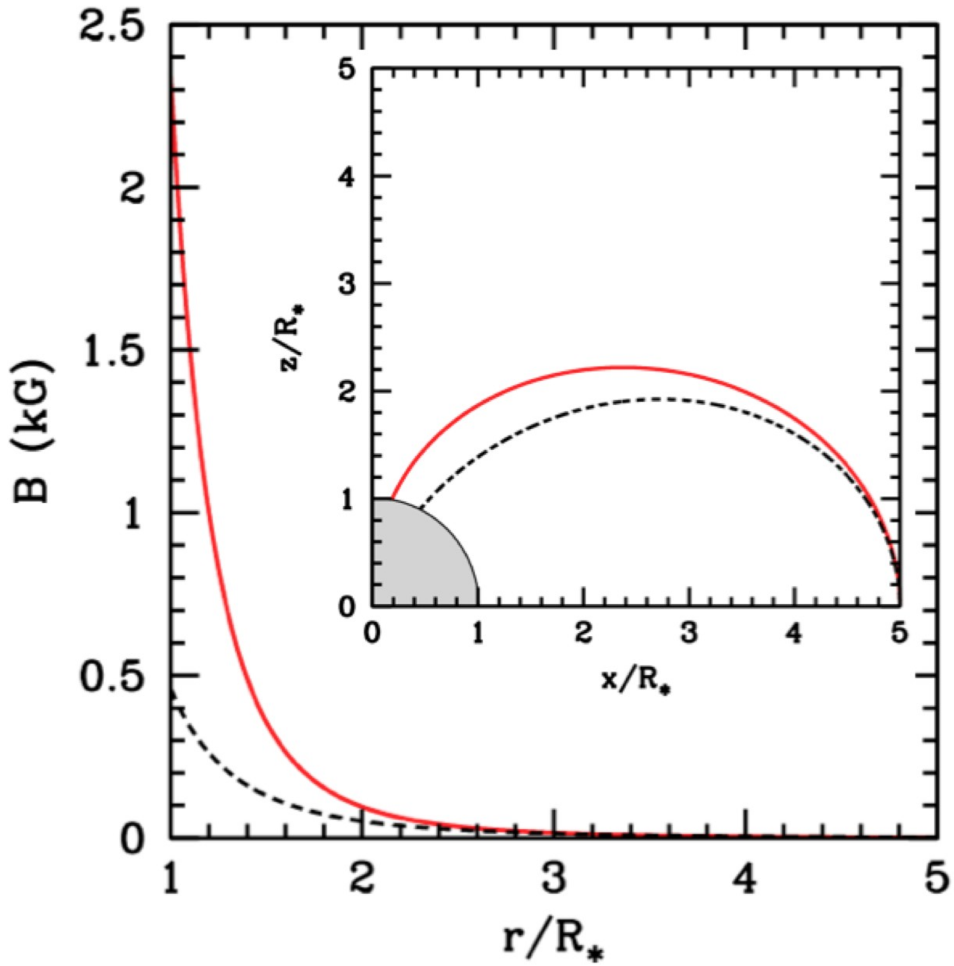

2.5
2
1.5
1
0.5
0
B (kG)
1
2
3
4
5
r/R*
z/R*
x/R*

Analytic multipole models

Multipole of order l, tilted by β relative to the stellar rotation axis, towards longitude ψ =(1-phase)*360o.

$$
\begin{aligned}
\mu_r &= \mu \sin\theta \cos\phi \cos\psi \sin\beta + \mu \sin\theta \sin\phi \sin\psi \sin\beta + \mu \cos\theta \cos\beta \\
\mu_\theta &= \mu \cos\theta \cos\phi \cos\psi \sin\beta + \mu \cos\theta \sin\phi \sin\psi \sin\beta - \mu \sin\theta \cos\beta \\
\mu_\phi &= -\mu \sin\phi \cos\psi \sin\beta + \mu \cos\phi \sin\psi \sin\beta.
\end{aligned}
$$

$$
\mathbf{B} = \frac{B_*^{\ell,pole}}{(\ell+1)} \left(\frac{R_*}{r}\right)^{\ell+2} \sum_{k=0}^{N} \left\{ \frac{(-1)^k (2\ell-2k)!}{2^\ell k!(\ell-k)!(\ell-2k)!} (\hat{\boldsymbol{\mu}} \cdot \hat{\mathbf{r}})^{\ell-2k} \left[(2\ell-2k+1)\hat{\mathbf{r}} - (\ell-2k)(\hat{\boldsymbol{\mu}} \cdot \hat{\mathbf{r}})^{-1} \hat{\boldsymbol{\mu}} \right] \right\}
$$

where $N = \ell/2$ or $N = (\ell-1)/2$ whichever is an integer.

(Gregory et al 2010; Gregory & Donati 2011)

V2129 Oph: Jul09 (upper) Jun05 (lower)

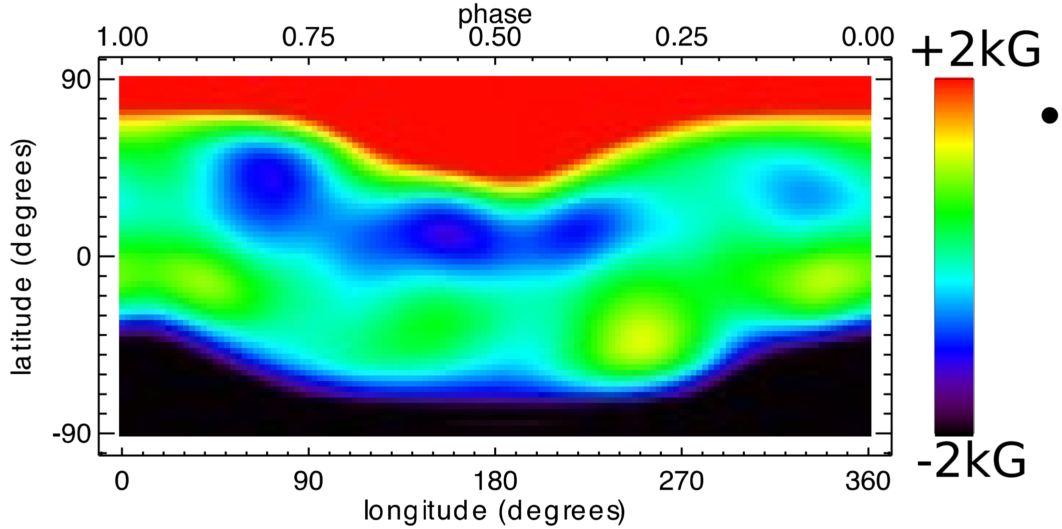

- Evidence for field evolution between observing epochs (e.g. Donati et al 2011a)

- Boct/Bdip ~ 2.9 (2.2) in 2005 (2009). Dipole component more than twice as strong in 2009.